Inorganic Chemistry

ARTICLE

pubs.acs.org/IC

Synthesis of Blue Imino(pentafluorophenyl)phosphane

Marcus Kuprat,[†] Mathias Lehmann,[†] Axel Schulz,[*,†,‡] and Alexander Villinger[†]

[†]Universität Rostock Institut für Chemie, Albert-Einstein-Strasse 3a, 18059 Rostock, Germany

[‡]Leibniz-Institut für Katalyse e.V. an der Universität Rostock, Albert-Einstein-Strasse 29a, 18059 Rostock, Germany

Supporting Information

ABSTRACT: The reaction of AgC_6F_5 with monomeric iminophosphanes of Mes*−N═P−X (X = Cl, I) in CH_2Cl_2 at ambient temperature gives imino(pentafluorophenyl)phosphane, Mes*N═P(C_6F_5) (**1**), in almost quantitative yield (96%), which could be isolated as a highly viscous blue oil. The same reaction with LiC_6F_5 results in the formation of imino(amino)phosphane (C_6F_5)$_2$P−N(Mes*)−P═NMes* (**2**) (yield 93%). In the second series of experiments the analogous reaction of MC_6F_5 (M = Ag, Li) with dimeric [Cl−P(μ-N−Dipp)]$_2$ was studied, leading to the formation of [R−P(μ-N−Dipp)]$_2$ (R = C_6F_5) (**3**) for M = Ag, while only decomposition products such as P(C_6F_5)$_3$ were observed in the reaction with the Li salt. Highly labile Mes*−N═P−C_6F_5 (**1**) decomposes at ambient temperatures, forming among other products the diphosphane (C_6F_5)$_2$P−P(C_6F_5)$_2$ (**4**). Reaction of **1** with $Fe_2(CO)_9$ yields the iron carbonyl complexes Mes*−N═P(C_6F_5)·Fe(CO)$_4$ (**5**) and [Mes*−N═P(C_6F_5)]$_2$·Fe(CO)$_3$ (**6**). The structure, bonding, and potential energy surface are discussed on the basis of B3LYP/6-31G(d, p) computations. According to time-dependent B3LYP calculations, the blue color of **1** arises from an n → π^* electronic transition.

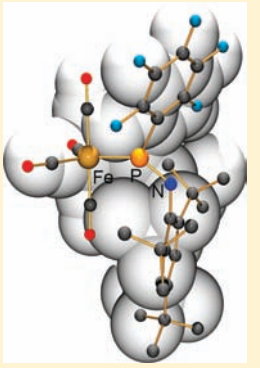

INTRODUCTION

The low coordination number chemistry of phosphorus−nitrogen compounds was extensively developed over the last four decades thanks to the use of bulky groups.[1,2] It has been possible to characterize these reactive PN species due to their kinetic and thermodynamic stabilization by appropriate substitution.

It was not until 1973 that Flick and Niecke were able to isolate a phosphorus(III)−nitrogen compound with the structural feature of a phosphazene, −P═N−.[3] This first iminophosphane, a phosphazene with phosphorus in coordination number two, was yielded from the reaction of bis(trimethylsilyl)aminodifluorophosphane with lithium−bis(trimethylsilyl)amide (eq 1)

$$(Me_3Si)_2N{-}PF_2 + LiN(SiMe_3)_2 \rightarrow (Me_3Si)_2N{-}P{=}N{-}SiMe_3 + LiF + Me_3Si{-}F \quad (1)$$

Monomeric halogeno(imino)phosphanes, R−N═P−X (X = halogen), have been isolated only for derivatives involving the bulky Mes* (Mes* = 2,4,6-tri-*tert*-butylphenyl) substituent at nitrogen,[4] which imposes a relative destabilization of the corresponding dimer due to substituent steric strain.[5] Slightly smaller substituents attached at the nitrogen atom such as the Dipp group (Dipp = 2,6 diisopropylphenyl) lead to 1,3-dihalogenocyclo-1,3-diphospha-2,4-diazanes.[6] The electronic and kinetic reasons for this R−N═P−X/[ClP(μ-NR)]$_2$ dimerization process have been addressed recently.[7] Furthermore, it is known that electron-rich iminophosphanes of the type R−N═P−R (R = aryl, alkyl) can dimerize in a [2 + 1] cycloaddition (Scheme 1).

Today, compounds bearing NP bonds are extensively studied inorganic species,[2−5,8] and a vast body of structural and spectroscopic data is available. However, much less is known about iminophosphane compounds containing the pentafluorophenyl group.[8e] Herein, we report on the synthesis of pentafluorophenyl-substituted iminophosphanes and their iron carbonyl complexes.

RESULTS AND DISCUSSION

Synthesis. Monomeric iminophosphanes of the type R−N═P−X (X = halogen) are only known for R = Mes*. Thus, it was of interest to study if it is possible to substitute the halogen X by the formal pseudohalogen pentafluorophenyl. The halogen/C_6F_5 substitution was attempted by means of the silver and the lithium C_6F_5 salts, MC_6F_5 (M = Ag, Li), as illustrated in Scheme 2. Surprisingly, only the reaction of AgC_6F_5 in CH_2Cl_2 at RT gives the desired product Mes*−N═P−C_6F_5 (**1**) in almost quantitative yield (96%), while 1,1-bis(pentafluorophenyl)-2,4-bis(2,4,6-tri-*tert*-butylphenyl)-1,3-diphospha-2,4-diazene, (C_6F_5)$_2$P−N(Mes*)−P═N−Mes* (**2**), was obtained in the reaction of LiC_6F_5 with Mes*−N═P−Cl in diethyl ether (yield 93%). While the synthesis of **1** can be carried out at ambient temperatures, in the case of **2**, the reaction was carried out at −80 °C and then slowly warmed to ambient temperatures over a period of 1 h. Obviously, the Lewis-acidic metal center plays an important role. Since the silver iodide and chloride, respectively, are sparingly soluble in contrast to lithium chloride, it can be assumed that formation of **2** is mediated by solvated Li^+ species.

In a second series of experiments we studied the analogous reaction of MC_6F_5 (M = Ag, Li) with dimeric [Cl−P(μ-N−Dipp)]$_2$ (**3Cl**) in order to investigate if there are also

Received: March 26, 2011
Published: May 25, 2011

Scheme 1. Different Channels for the Dimerization of $R_1-N{=}P-R_2$

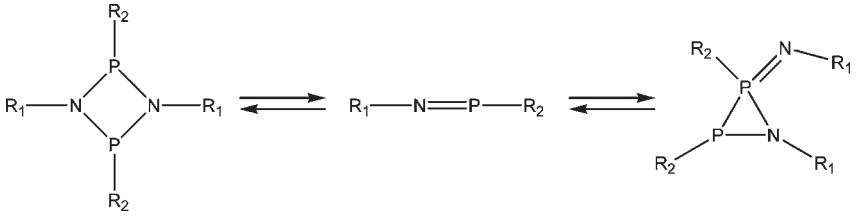

Scheme 2. Reaction of Mes*−N═P−X with MC_6F_5 (M = Ag, Li)

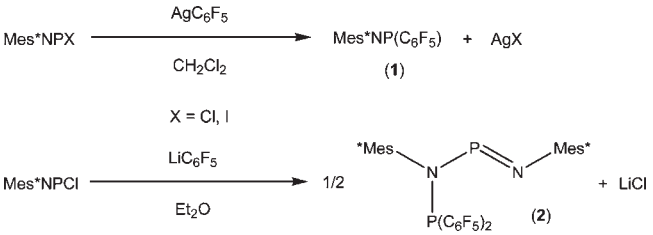

Scheme 3. Reaction of $[Cl-P(\mu\text{-}N-Dipp)]_2$ with AgC_6F_5

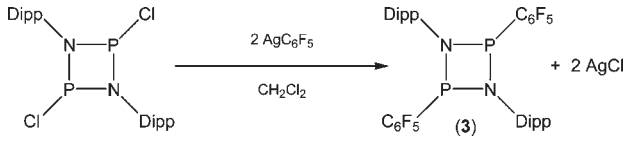

different reaction channels for the Cl/C_6F_5 substitution depending on the used metal. Indeed, two different reaction pathways were detected too. While the reaction with the silver salt in CH_2Cl_2 at −80 °C yielded the expected 1,3-bis(pentafluorophenyl)-2,4-bis(2,6-di-isopropylphenyl)-cyclo-1,3-diphospha-2,4-diazene $[DippNP(C_6F_5)]_2$ (**3**) (yield 65%, Scheme 3), only decomposition products such as $P(C_6F_5)_3$, characterized by X-ray structure elucidation, were obtained from the reaction with LiC_6F_5 in diethyl ether at −80 °C, which is followed by a slow warming up. Even better yields for **3** and less side products are obtained when the iodine species, $[I-P(\mu\text{-}N-Dipp)]_2$ (**3I**), is used. Moreover, the halogen/C_6F_5 substitution is much faster when the iodine species is utilized. To the best of our knowledge $[DippNP(C_6F_5)]_2$ (**3**) has not been described yet.

Properties and Characterization. Mes*−N═P−C_6F_5 (**1**) can be isolated as a highly viscous, deep blue liquid in contrast to **2**, which is an orange crystalline solid. The blue color is rather unusual taking into account that the vast majority of PN species are either yellow or red colored but has already been observed by Burford et al. for a solution of in-situ-prepared Mes*−N═P−C_6H_5 in CH_2Cl_2.[9] The UV−vis spectrum of the deep blue CH_2Cl_2 solution of **1** exhibits one very weak characteristic n → π^* electronic transition at 592 nm (besides strong $\pi \rightarrow \pi^*$ electronic transitions in the range <380 nm), which could be assigned on the basis of TD-B3LYP calculation (Tables S11, see Supporting Information). The blue color arises from the weak n → π^* HOMO−LUMO electronic transition (Figure 1). The HOMO describes a delocalized mainly

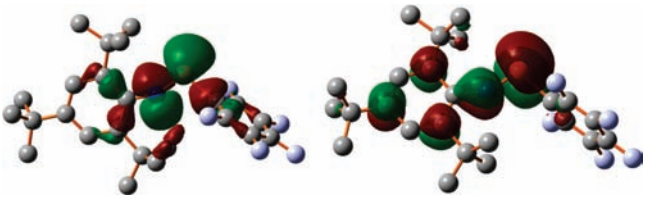

Figure 1. HOMO and LUMO in **1**.

Table 1. ^{31}P NMR Data (chemical shift in ppm) and Selected Structural Data (distances in Angstroms, angles in degrees) of Amino(imino)phosphanes of the Type $R^1R^2N-P{=}N-Mes^*$,[a] 1, 2, Mes*−N═P−Cl, and $Mes^*NP^+AlCl_4^-$

R^1, R^2	P═N	PNC	^{31}P shift
H, Mes*[d]	1.573(8)	126.1(7)	272
Me_3Si, Me_3Si[d]	1.566(2)	117.6(2)	327
*i*Pr, *i*Pr[d]	1.555(2)	129.6(2)	268
Me, Me[d]	1.538(3)	140.7(4)	203
Mes*−N═P−Cp* (trans)[d]	1.552(5)	125.9(4)	194
^{t}Bu−N═P−Mes*[d]	1.556(5)	122.7(5)	
Mes*−N═P−^{t}Bu[d]			490
1[b]	1.565	153.2	363
2	1.541(2)	133.6(2)	11.5, 290
Mes*−N═P−I[d]	1.480(3)	172.5(3)	218
Mes*−N═P−Br[d]	1.499(6)	161.0(6)	153
Mes*−N═P−Cl[c]	1.506(2)	146.7(2)	139
Mes*−N═P−F[d]			87
$Mes^*NP^+AlCl_4^-$[c]	1.475(8)	177.0(7)	79

[a] Taken from ref 11. [b] Calculated values at the B3LYP/6-31G(d,p) level of theory. [c] Taken from ref 4 or 12. [d] Taken from ref 2.

nonbonding molecular orbital with large coefficients along the C−N−P−C unit, while the LUMO displays an antibonding PN π^* bond.

Furthermore, **1** was characterized by elemental analysis, Raman/IR, and NMR spectroscopy as well as mass spectrometry (ESI-TOF/MS: 457 $[Mes^*-N{=}P-C_6F_5]^+$). The ^{31}P NMR spectrum of **1** displayed one singlet resonance at δ = 361.6, which is shifted to low field compared to the two resonances found for **2**, which are observed at δ = 11.49 (m, *P*NP) and 290.15 (d, $^2J(^{31}P-^{31}P)$ = 6.7 Hz, *N*PN), respectively. For comparison, the ^{31}P NMR shift of Mes*−P═N−Cl is found at δ = 139 and for $[Mes^*-N{\equiv}P]^+$ at δ = 79.[4] ^{31}P NMR data of several PN species are summarized in Table 1. From these data it can be concluded that the ^{31}P NMR resonance is observed at low field the more

dx.doi.org/10.1021/ic200623x |*Inorg. Chem.* 2011, 50, 5784–5792

Scheme 4. Synthesis of 4

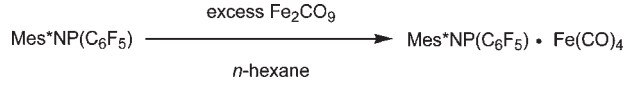

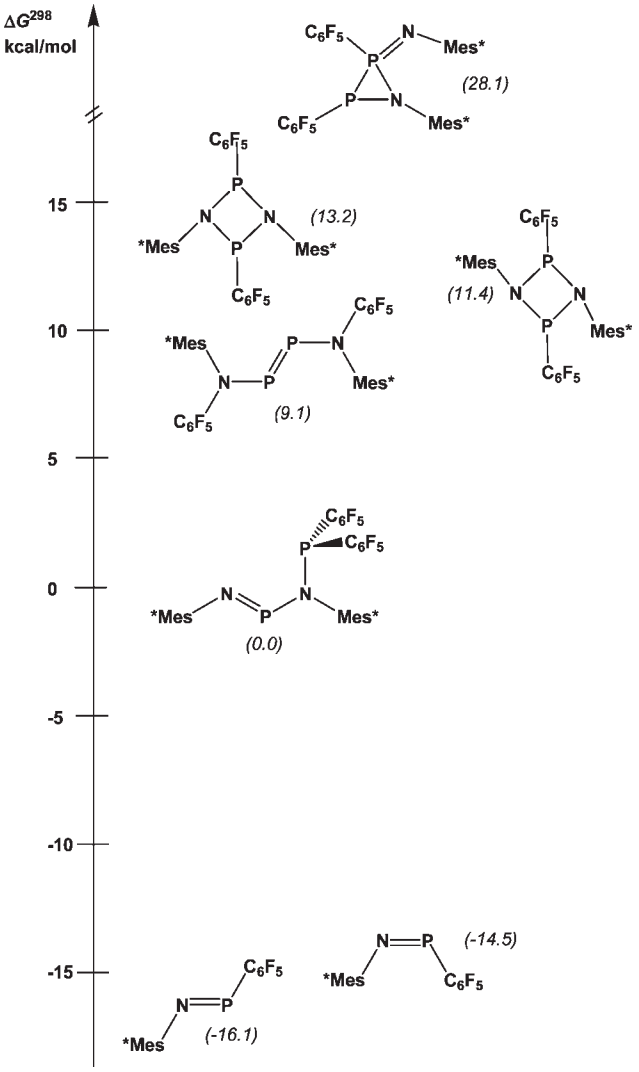

Figure 2. Relative Gibbs energies for the isomers of $[Mes^*NP(C_6F_5)]_y$ (y = 1, 2). The exact values are given in parentheses.

electron rich the PN unit is and vice versa (cf. R−N=P−X; X = I, 210; Br, 153; Cl, 139; F, 87; $[RNP]^+$ = 79 ppm; R = Mes*).

In contrast to **2**, which is thermally stable at ambient temperatures (Mp 123 °C), compound **1** is thermally labile, moisture sensitive, but stable under argon atmosphere over a long period at low temperatures (−80 °C) as a solid but slowly decomposes in benzene solution. Both compounds (**1** and **2**) can be prepared in bulk. This together with the very good solubility in common organic solvents makes both compounds good precursors for further synthesis.

Slow decomposition of **1** is already observed at ambient temperatures. Thermal treatment of **1** up to 102 °C in vacuum (10^{-3}mbar) led to a fast decomposition yielding a yellow oil. Among the decomposition products diphosphane $(C_6F_5)_2P-P(C_6F_5)_2$ (**4**) could be isolated and characterized by X-ray single

Table 2. Calculated Selected Structural Data of *trans*-1, *cis*-1, 2, and Dimers of 1

	CN	NP	PC	CNP	NPC	CNPC
trans-**1**	1.370	1.565	1.903	153.2	103.8	180.0
cis-**1**	1.397	1.552	1.905	148.2	113.9	0.3
2	1.410	1.568	1.862	111.5	104.4	−22.3
	1.472	1.756	1.893	124.9	110.2	85.9
		1.780		131.9		
trans-dimer	1.437	1.772	1.899	119.6	102.3	−46.1
	1.437	1.763	1.900	119.6	102.8	−113.4
		1.764		134.9	106.4	48.6
		1.774		135.3	107.2	112.4
cis-dimer	1.444	1.757	1.918	122.3	104.8	−74.8
	1.451	1.763	1.920	122.9	106.8	−77.0
		1.764		138.2	108.2	61.3
		1.768		138.8	110.1	88.4

crystallography. Diphosphane $(C_6F_5)_2P-P(C_6F_5)_2$, which is easily prepared from the reaction of $(C_6F_5)_2PBr$ with mercury or magnesium, has already been reported,[10] but so far, its structural data have not been published yet.

Since it was impossible to obtain crystals of **1** suitable for single-crystal structure elucidation (even at low temperature), **1** was reacted with $Fe_2(CO)_9$ to obtain iron−carbonyl adducts. The iron carbonyl adduct formation reaction is straightforward and can easily be followed by ^{31}P NMR experiments. Upon addition of a solution of **1** in *n*-hexane to a stirred suspension of $Fe_2(CO)_9$ in *n*-hexane at −50 °C, an immediate reaction occurred leading to a brown suspension (Scheme 4). The suspension was slowly warmed to ambient temperatures. Filtration gave a dark red solution from which after concentration black crystals of $Fe_3(CO)_{12}$ were obtained. Decantation of the supernatant, further concentration, and storage at ambient temperature gave red crystals of *N*-(2,4,6-tri-*tert*-butylphenyl)imino-(pentafluorophenyl)phosphane iron tetracarbonyl adduct, $Mes^*NP(C_6F_5)\cdot Fe(CO)_4$ (**5**), which could be isolated in good yields (82%). It should be mentioned that $[Mes^*NP(C_6F_5)]_2\cdot Fe(CO)_3$ (**6**) was observed when no excess of $Fe_2(CO)_9$ was used.

Power et al. frequently used iron carbonyl complexes to stabilize element−element double bonds, e.g., diphosphenes, RP=PR.[13] For example, the reaction of $Na_2Fe(CO)_4$ with different bulky monosubstituted phosphorus(III) halides $RPCl_2$, where R = 2,4,6-$Me_3C_6H_2$, CH_2SiMe_3, $CH(SiMe_3)_2$, N-$(SiMe_3)_2$, $-OC_6H_2$-2,6-^{t}Bu$_2$-4-Me, or $-OC_6H_2$-2,4,6-^{t}Bu$_3$ yielded products in which the phosphorus center behaves as either a diphosphene or a bridging phosphinidene group. Complexes **5** and **6** are rare examples of iron carbonyl complexes featuring an iminophosphane as ligand.

Computations. Inspection of the conformational space at the B3LYP/6-31G(d,p) level of theory displayed two different monomeric structures for **1** (Figure 2): (i) a cis isomer (*cis*-**1**) and (ii) a trans arrangement (*trans*-**1**) with respect to the $C_{Mes^*}-N=P-C_{C6F5}$ moiety. Our calculation revealed that the trans−cis energy gap is rather small, with the trans form being the most stable isomer (ΔE^{tot}(cis−trans) = +0.1 kcal/mol, ΔG^{298}-(cis−trans) = 0.8 kcal/mol). Different dimerization processes must be considered. As shown in Figure 2, four different dimers were found: (i) a cyclic imino(amino)phosphane (**2**) with NPNP connectivity and a diphosphene[1a,14] with a NPPN

dx.doi.org/10.1021/ic200623x |*Inorg. Chem.* 2011, 50, 5784–5792

Table 3. Crystallographic Details of 2, 3Cl, 3I, and 3

	2	3Cl	3I	3
chemical formula	$C_{48.98}H_{59.96}Cl_{1.96}F_{10}N_2P_2$	$C_{30}H_{40}Cl_2N_2P_2$	$C_{24}H_{34}I_2N_2P_2$	$C_{60}H_{58}F_{10}N_2P_2$
fw [g mol^{-1}]	998.13	561.48		1059.02
color	orange	colorless	yellow	yellow
cryst syst	monoclinic	orthorhombic	triclinic	triclinic
space group	$P2_1/n$	$P2_12_12_1$	$P-1$	$P-1$
a [Å]	18.2786(7)	9.8933(3)	9.0746(3)	10.1554(4)
b [Å]	10.6517(4)	18.1268(6)	9.2454(3)	11.7132(4)
c [Å]	26.1221(10)	35.2455(11)	9.5949(4)	12.2055(5)
α [deg]	90.00	90.00	67.447(2)	108.513(2)
β [deg]	99.774(2)	90.00	83.782(2)	100.009(2)
γ [deg]	90.00	90.00	70.667(2)	93.573(2)
V [Å^3]	5012.1(3)	6320.7(3)	701.35(4)	1345.01(9)
Z	4	8	1	1
ρ_{calcd} [g cm^{-3}]	1.323	1.180	1.577	1.307
μ [mm^{-1}]	0.264	0.327	2.369	0.156
$\lambda_{MoK\alpha}$ [Å]	0.71073	0.71073	0.71073	0.71073
T [K]	173(2)	173(2)	173(2)	173(2)
measured reflns	44 100	76 995	22 552	39 880
independent reflns	11 440	15 223	4931	8513
reflns with $I > 2\sigma(I)$	8501	11 583	4108	6517
$R_{int.}$	0.0463	0.0692	0.0227	0.0315
$F(000)$	2085	2384	328	552
R_1 (R [$F^2 > 2\sigma(F^2)$])	0.0562	0.0445	0.0262	0.0434
wR_2 (F^2)	0.1445	0.0888	0.0672	0.1193
GooF	1.057	1.003	1.055	1.050
parameters	655	665	159	338

connectivity and (ii) two isomers for cyclo-diphosphadiazane besides a high-lying three-membered NPP heterocycle bearing P^{III} and P^{V} atoms. In agreement with experiment, all computed dimerization processes are endergonic (e.g., ΔG^{298}(**2** − 2 × *trans*-**1**) = +16.1 kcal/mol). It should be noted that at least dimerization to **2** represents an exothermic process (ΔG^{298}(**2** − 2 × *trans*-**1**) = −3.3 kcal/mol, see Table S10 in the Supporting Information).

Since it was impossible to obtain experimental structural data for **1**, its structure was calculated for the gas phase at the B3LYP level of theory. Selected structural data of *trans*-**1** and *cis*-**1** along with data of different dimers are summarized in Table 2. The most interesting structural features of aryl-substituted iminophosphanes are the short PN double bond and rather large CNP angles. While for *trans*-**1** and *cis*-**1** the PN distances of 1.555 and 1.552 Å, respectively, are fairly similar and in the expected range (cf. Σr_{cov}(P═N) = 1.52 Å),[15] the C_{Mes^*}−N distance in *trans*-**1** (1.370 Å) is significantly shorter compared to that in *cis*-**1** (1.397 Å). Since for both species the CNPC unit is planar and allows delocalization of the 6π aryl electrons, the computed difference in the CN bond can be attributed to a larger steric strain in *cis*-**1**. In both species the C_6F_5 ring adopts a perpendicular position to the Mes* ring.

MO and NBO[16] calculations for **1** displayed highly polarized P−N and P−C bonds. While for the P−C bond only 31% of the NBO electron density is localized at the P atom, for the P−N σ bond this value is further decreased to 24% but increased for the π bond to 39%. The hybrid orbital at the P atom used for the P−C bond possesses 12% s atomic orbital character, which increases to 17% in the P−N bond. The calculated natural atomic orbital population (NAO) net charges are q = +0.14 (C_{Mes^*}), −0.85 (N), +0.96 (P), and −0.49 e (C_{C6F5}) and alternate along the C_{Mes^*}−N−P−C_{C6F5} unit. Charge comparison of the PN unit in **1** with neutral PN (q(P) = +0.77, q(N) = −0.77e) shows a charge transfer of only 0.10e, although the entire Mes* group donates 0.41 electrons of which, however, 0.30 electrons are accepted by the C_6F_5 group, describing a formal classic push−pull situation.[2]

X-ray Crystallography. The structures of compounds **2**−**6** have been determined. Tables 3 and 4 present the X-ray crystallographic data. Selected molecular parameters are listed in Figures 3−8. X-ray quality crystals of all considered species were selected in Kel-F-oil (Riedel deHaen) or Fomblin YR-1800 (Alfa Aesar) at ambient temperatures. All samples were cooled to −100(2) °C during the measurement.

Mes*N═P−N(Mes*)−P(C_6F_5)$_2$ (**2**) crystallizes in the triclinic space group P-1 with two formula units per cell. The structure consists of separated Mes*N═P−N(Mes*)−P(C_6F_5)$_2$ and triply disordered CH_2Cl_2 molecules with no significant intermolecular contacts. In contrast to the trigonal pyramidal P2 atom, both nitrogen atoms and the dicoordinated P1 atom sit in a trigonal planar environment with a PN double bond of 1.541(2) Å (P1−N1) and two PN single bonds of 1.726(2) (P1−N2) and 1.740(2) Å (P2−N2), respectively, which lies in the expected range for amino(imino)phosphanes, for example, P═N 1.545(6) Å and P−N 1.632(6) Å in MeN(H)−P═N−Mes* (Σr_{cov}(P−N) = 1.76 Å and Σr_{cov}(P═N) = 1.52 Å).[2,10,13]

Since the phenyl ring of the Mes* group attached to N1 lies orthogonal to the plane composed of N1, P1, N2, and P2 there is

dx.doi.org/10.1021/ic200623x |*Inorg. Chem.* 2011, 50, 5784–5792

Table 4. Crystallographic Details of 4, 5, and 6

	4	5	6
chemical formula	$C_{24}F_{20}P_2$	$C_{28}H_{29}F_5FeNO_4P$	$C_{51}H_{58}F_{10}FeN_2O_3P_2$
fw [g mol^{-1}]	730.18	625.34	1054.78
color	colorless	red	red
cryst syst	tetragonal	triclinic	monoclinic
space group	P-42$_1$c	P-1	$P2_1/n$
a [Å]	12.9649(16)	8.6162(3)	20.3424(6)
b [Å]	12.9649(16)	10.4409(3)	22.6247(7)
c [Å]	42.228(12)	17.9784(6)	24.7584(8)
α [deg]	90.00	93.508(2)	90.00
β [deg]	90.00	98.424(2)	112.2600(10)
γ [deg]	90.00	113.3970(10)	90.00
V [Å^3]	7098(2)	1455.60(8)	10545.6(6)
Z	12	2	8
ρ_{calcd} [g cm^{-3}]	2.050	1.427	1.329
μ [mm^{-1}]	0.359	0.639	0.424
$\lambda_{MoK\alpha}$ [Å]	0.71073	0.71073	0.71073
T [K]	173(2)	173(2)	173(2)
measured reflns	19 726	48 927	77 741
independent reflns	5223	10 458	18 565
reflns with $I > 2\sigma(I)$	3834	8133	9788
$R_{int.}$	0.0542	0.0331	0.1054
$F(000)$	4248	644	4384
R_1 (R [$F^2 > 2\sigma(F^2)$])	0.0486	0.0339	0.0520
wR_2 (F^2)	0.1045	0.0958	0.1101
GooF	1.073	1.049	0.919
parameters	622	401	1320

no interaction between the PN π bond and the π system of the phenyl ring (Figure 3). A look along the N1, P1, N2, and P2 unit displays a cis conformation and an almost planar arrangement of all four atoms (N1−P1−N2−P2 13.6(2)°). While a rather small angle is found around the dicoordinated P1 atom (N1−P1−N2 108.47(9)°), due to steric repulsion the angle around the dicoordinated N1 atom is fairly large with 133.6(2)° (C1−N1−P1).

Mes*NP(C_6F_5)·Fe(CO)$_4$ (**5**) crystallizes in the space group $P\bar{1}$ with two molecules per unit cell. The perspective view of the complex is illustrated in Figure 4. The primary coordination sphere consists of an iron-centered trigonal bipyramidal arrangement of the four CO ligands and the *trans*-Mes*−N═P−C_6F_5 ligands (C_{axis}−Fe−C/P_{plane} angles between 89.8° and 91.4°, axis: C28−Fe−C25 178.19(5), trigonal plane: C27−Fe−C26 115.08(7)°, C27−Fe−P 122.33(5)°, C26−Fe−P 122.58(5)°). Seven CO···F−C intermolecular interactions with three different Mes*−N═P−(C_6F_5) ligands are observed besides numerous C−F···H−C contacts. The O···F distances between 2.802(1) (O1···F2′) and 3.000(2) Å (O1···F3′), respectively, lie within the range of weak F···O van der Waals interactions (cf. Σr_{vdW}(F−O) = 3.0 Å).[13] Due to these van der Waals interactions, in the crystal the iron complexes are arranged in such a manner that stacked chains of alternating polar "Fe(CO)$_4$-units" and nonpolar "Mes*-units" are formed.

The Mes*−N═P−C_6F_5 ligand is part of the trigonal plane and attached to the iron atom via the phosphorus with a Fe−P bond length of 2.1225(3) Å (cf. 2.232 (l) Å in the diphosphene iron carbonyl complex (CO)$_4$Fe−P(R)═P(R)−Fe(CO)$_4$, R = N(SiMe$_3$)$_2$).[17] The P−N distance in **2** (1.558(1) Å) is found in the range expected for the free ligand (calculated value for the gas-phase species 1.565 Å, in Mes*N═P−N(Mes*)−P(C_6F_5)$_2$ (**2**) 1.541(2) Å). This is probably due to the fact that the HOMO (Figure 1) represents a nonbonding molecular orbital with a large coefficient at the P atom. Thus, this MO describes

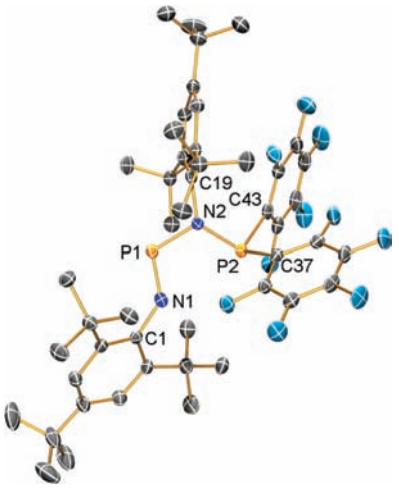

Figure 3. ORTEP drawing of the molecular structure of **2** in the crystal. Thermal ellipsoids with 50% probability at 173 K (hydrogen atoms omitted for clarity). Selected bond lengths (Å) and angles (deg): P1−N1 1.541(2), P1−N2 1.726(2), P2−N2 1.740(2), P2−C43 1.846(2), P2−C37 1.872(2), N1−C1 1.419(3), N2−C19 1.473(3); N1−P1−N2 108.47(9), N2−P2−C43 104.09(9), N2−P2−C37 109.61(9), C43−P2−C37 101.1(1), C1−N1−P1 133.6(2), C19−N2−P1 111.5(1), C19−N2−P2 125.8(1), P1−N2−P2 120.7(1), N1−C1−C6 117.0(2), N1−C1−C2 124.2(2), C38−C37−P2 128.6(2), C42−C37−P2 115.6(2), C48−C43−P2 128.5(2), C44−C43−P2 115.9(2), N2−P1−N1−C1 −174.1(2), N1−P1−N2−C19 178.5(1), N1−P1−N2−P2 13.6(2).

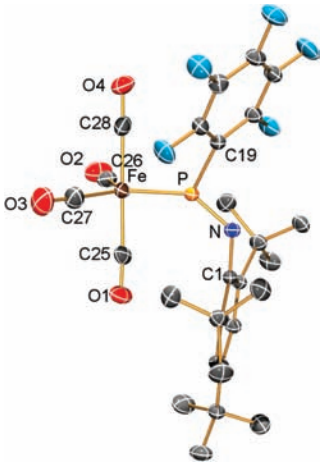

Figure 4. ORTEP drawing of the molecular structure of **5** in the crystal. Thermal ellipsoids with 50% probability at 173 K (hydrogen atoms omitted for clarity). Selected bond lengths (Å) and angles (deg): P−N 1.558(1), P−C19 1.825(1), P−Fe 2.1225(3), N−C1 1.417(1), Fe−C28 1.803(1), Fe−C27 1.804(1), Fe−C26 1.812(1), Fe−C25 1.819(1), O1−C25 1.130(2), O2−C26 1.135(2), O3−C27 1.141(2), O4−C28 1.134(2); N−P−C19 101.66(5), N−P−Fe 138.80(4), C19−P−Fe 119.52(4), C1−N−P 125.47(8), C28−Fe−C27 90.09(6), C28−Fe−C26 90.32(6), C27−Fe−C26 115.08(7), C28−Fe−C25 178.19(5), C27−Fe−C25 89.78(6), C26−Fe−C25 91.38(5), C28−Fe−P 88.84(4), C27−Fe−P 122.33(5), C26−Fe−P 122.58(5), C25−Fe−P 89.71(4), C19−P−N−C1 177.23(9).

mainly the lone pair localized at the P atom in the Lewis picture. The steric effects of binding Fe(CO)$_4$ to the Mes*−N═P−C_6F_5 species in **4** is reflected in the position (trigonal plane) and orientation of the Mes* and C_6F_5 aryl rings. Both rings and the

dx.doi.org/10.1021/ic200623x |*Inorg. Chem.* 2011, 50, 5784–5792

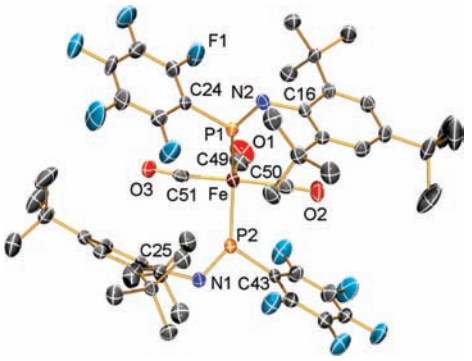

Figure 5. ORTEP drawing of the molecular structure of **6** in the crystal. Thermal ellipsoids with 50% probability at 173 K (hydrogen atoms omitted for clarity). Selected bond lengths (Å) and angles (deg): Fe1−C49 1.803(4), Fe1−C51 1.816(4), Fe1−C50 1.819(4), Fe1−P1 2.133(1), Fe1−P2 2.134(1), P1−N2 1.562(3), P1−C19 1.833(3), P2−N1 1.566(3), P2−C43 1.830(3), N1−C25 1.419(4), N2−C1 1.425(4); C49−Fe1−C51 92.9(2), C49−Fe1−C50 93.8(2), C51−Fe1−C50 173.3(2), C49−Fe1−P1 111.9(1), C51−Fe1−P1 87.1(1), C50−Fe1−P1 89.6(1), C49−Fe1−P2 110.1(1), C51−Fe1−P2 91.9(1), C50−Fe1−P2 86.6(1), P1−Fe1−P2 137.98(4), N2−P1−C19 101.5(2), N2−P1−Fe1 137.5(1), C19−P1−Fe1 120.9(1), N1−P2−43 101.9(2), N1−P2−Fe1 138.1(1), C43−P2−Fe1 119.8(1), C25−N1−P2 121.3(2).

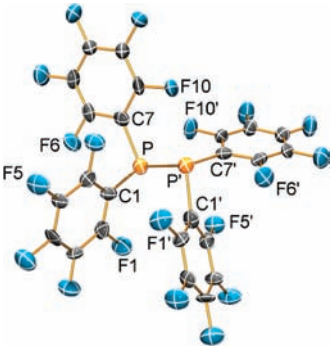

Figure 6. ORTEP drawing of the molecular structure of **4** in the crystal. Thermal ellipsoids with 50% probability at 173 K (hydrogen atoms omitted for clarity). Selected bond lengths (Å) and angles (deg): P1−C7 1.848(6), P1−C1 1.868(6), P1−P1^{i} 2.248(3); C7−P1−C1 99.9(3), C7−P1−P1^{i} 102.8(2), C1−P1−P1^{i} 95.0(2). Symmetry codes: (′) $-x, -y + 1, z$.

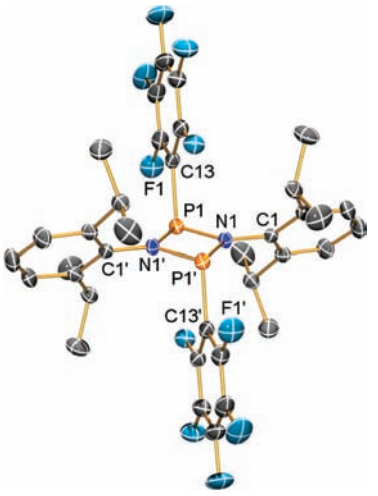

Figure 7. ORTEP drawing of the molecular structure of **3** in the crystal. Thermal ellipsoids with 50% probability at 173 K (hydrogen atoms omitted for clarity). Selected bond lengths (Å) and angles (deg): P1—N1 1.7204(9), P1—N1^{i} 1.7225(9), P1—C13 1.874(1), P1—P1^{i} 2.6173(5), N1—C1 1.427(1), N1—P1^{i} 1.7225(9), N1—P1—N1^{i} 81.04(4), N1—P1—C13 105.09(5), P1—N1—P1^{i} 98.96(4). Symmetry codes: (′) $1 - x, 1 - y, 1 - z$.

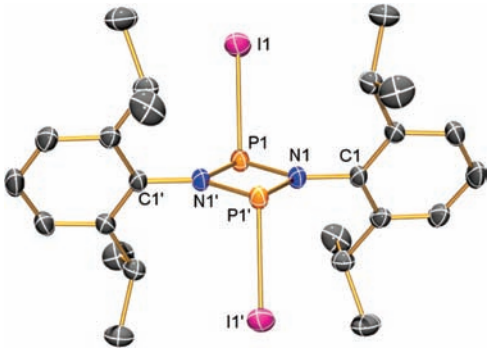

Figure 8. ORTEP drawing of the molecular structure of **3I** in the crystal. Thermal ellipsoids with 50% probability at 173 K (hydrogen atoms omitted for clarity). Selected bond lengths (Å) and angles (deg): P1—N1 1.697(1), P1—N1^{i} 1.714(1), P1—P1^{i} 2.5894(8), N1—C1 1.430(2), N1—P1—N1^{i} 81.19(6), N1—P1—I1 104.38(5), N1^{i}—P1—I1 103.83(5), P1—N1—P1^{i} 98.81(6). Symmetry codes: (′) $1 - x, 1 - y, 1 - z$.

almost planar C1−N−P−C19 unit (C19−P−N−C1 177.23(9)°) are oriented parallel to the $Fe(CO)_4$ fragment.

$[Mes^*NP(C_6F_5)]_2 \cdot Fe(CO)_3$ (**6**) crystallizes in the monoclinic space group $P2_1/n$ with eight formula units (two independent molecules) per cell. In contrast to **2**, only one CO···F−C intermolecular interaction is observed (2.713(3) Å). With respect to bond lengths and angles similar structural features are found for the tricarbonyl iron complex **6** in comparison to the tetracarbonyl iron complex **5**: (i) The molecular structure also displays a slightly distorted trigonal bipyramidal iron center with the two Mes*−N═P−C_6F_5 ligands occupying a position in the trigonal plane. (ii) Both Mes−*N═P−C_6F_5 ligands are attached via the P atom (Fe1−P1 2.133(1) Å, Fe1−P2 2.134(1) Å). (iii) The Mes*−N═P−C_6F_5 ligands adopt a trans configuration with an almost planar C−P−N−C unit (C19−P1−N2−C1 178.8(3)° and C25−N1−P2−C43 177.0(2)°). (iv) Both PN bond lengths (P2−N1 1.566(3) Å, P1−N2 1.562(3) Å) are found in the expected range for a typical double bond (cf. Σr_{cov}(P═N) = 1.52 Å).

Diphosphane $(C_6F_5)_2P-P(C_6F_5)_2$ (**4**) crystallizes in the tetragonal space group $P\text{-}42_1c$ with 12 formula units per cell (three independent molecules). The structure consists of separated $(C_6F_5)_2P-P(C_6F_5)_2$ molecules with no significant intermolecular contacts. The main feature of interest is the P−P distance of 2.248(3) Å, which is slightly longer than the sum of the covalent radii 2.2 Å. This slight increase is expected in view of the electronegative C_6F_5 moiety reducing the electron density in the bonding orbitals of the P−P unit. Both PR_2 fragments adopt a C_2-symmetric staggered configuration to each other.

dx.doi.org/10.1021/ic200623x |*Inorg. Chem.* 2011, 50, 5784–5792

Four-membered rings of the type $[X-P(\mu\text{-}NR)]_2$ containing alternating phosphorus(III) and nitrogen centers are known as cyclo-1,3-diphospha(III)-2,4-diazanes (X = halogen, R = organic group).[6,18,19] Cyclo-diphospha(III)-diazane $[Cl-P(\mu\text{-}NDipp)]_2$ was first generated by Burford et al. in the reaction of PCl_3 with $DippNH_2$.[20] Structural data of $[X-P(\mu\text{-}NR)]_2$ (X = I and C_6F_5, R = organic substitutent) have not been published to date. While compounds **3** and **3I** crystallize in the triclinic space group *P*-1 with one molecule per unit cell, for **3Cl** the orthorhombic space group $P2_12_12_1$[19] was found. Noteworthy, both **3** and **3Cl** crystallize with four and eight benzene molecules per unit cell, while no solvent is found for **3I**.

The molecular structures of **3** and **3I** (Figures 7 and 8) display trans-substituted centrosymmetric dimers with a planar P_2N_2 core protected by two bulky Dipp groups. The metrical parameters of the P_2N_2 core such as the N−P−N′ and P−N−P′ angles (NPN′ = 81.0−81.5°; PNP′ = 97.5−99.0°) do not change in **3**, **3Cl**, and **3I** and are in the same range found for $[X-P(\mu\text{-}NR)]_2$ (X = halogen, R = organic substituent).[19] Two slightly different P−N bond lengths between 1.697(1) and 1.7225(9) Å are found in the expected range for a typical single bond (cf. $\Sigma r_{cov}(P-N)$ = 1.76 Å). The P···P distances between 2.56 and 2.62 Å are slightly longer than the sum of the covalent radii (2.20 Å) but significantly shorter than the sum of the van der Waals radii (3.8 Å).[13] Thus, strong van der Waals interactions across the ring can be assumed.

CONCLUSION

Imino(pentafluorophenyl)phosphane, $Mes^*N{=}P(C_6F_5)$, was obtained in the reaction of AgC_6F_5 with monomeric iminophosphanes of Mes*−N═P−X (X = Cl, I). In contrast to the halogen-substituted Mes*−N═P−X, which are orange solids, $Mes^*N{=}P(C_6F_5)$ is a highly viscous blue oil (decomposition at 102 °C). The blue color arises from the weak n → π^* HOMO −LUMO electronic transition, with both MOs mainly localized along the PN unit.

A totally different reaction channel is observed when LiC_6F_5 was used instead of the silver salt, leading to formation of $(C_6F_5)_2P-N(Mes^*)-P{=}N-Mes^*$. When the Dipp substitutent was used instead of Mes*, again two different final products were isolated depending on the used metal in MC_6F_5 (M = Li, Ag). Dimeric $[C_6F_5-P(\mu\text{-}N-Dipp)]_2$ (R = C_6F_5) was isolated with AgC_6F_5. As expected, the Dipp substituent provides less steric strain which is not compensated by a strong push−pull system caused by the C_6F_5/Mes* substituents. Hence, only the dimer $[C_6F_5-P(\mu\text{-}N-Dipp)]_2$ is observed, in contrast to monomeric $Mes^*N{=}P(C_6F_5)$, in accord with theory.

Reaction of $Mes^*N{=}P(C_6F_5)$ with $Fe_2(CO)_9$ yields the hitherto unknown iron carbonyl complexes $Mes^*-N{=}P(C_6F_5)\cdot Fe(CO)_4$ and $[Mes^*-N{=}P(C_6F_5)]_2\cdot Fe(CO)_3$.

EXPERIMENTAL DETAILS

Synthesis of *N*-(2,4,6-Tri-*tert*-butylphenyl)imino(pentafluorophenyl)phosphane $Mes^*NP(C_6F_5)$ (1). To a stirred solution of Mes*NPX (X = Cl 0.160 g, 0.68 mmol, X = I 0.284 g, 0.68 mmol) in CH_2Cl_2 (5 mL) a suspension of AgC_6F_5 (0.192 g, 0.70 mmol) in CH_2Cl_2 (7 mL) is added dropwise at −80 °C over a period of 20 min. The resulting dark blue suspension is stirred for 10 min and then slowly warmed to ambient temperatures over a period of 1 h. The solvent is removed in vacuo, and the residue is extracted with *n*-hexane (10 mL) and filtered. Removal of solvent and drying in vacuo yields for X = Cl 0.256 g (0.559 mmol, 82%) and for X = I 0.299 g (0.653 mmol, 96%) of *N*-(2,4,6-tri-*tert*-butylphenyl)imino(pentafluorophenyl)phosphane $Mes^*NP(C_6F_5)$ (**1**) as a blue oil.

Decomposition at 102 °C. Anal. Calcd (found) for $C_{24}H_{29}F_5NP$ (457.46): C, 63.01 (61.23); H, 6.39 (5.98); N, 3.06 (2.98). ^{1}H NMR (25 °C, CD_2Cl_2, 300.13 MHz): δ = 1.35 (s, 9 H, *p*-C(CH_3)$_3$), 1.37 (s, 18 H, *o*-C(CH_3)$_3$), 7.41 (d, 2 H, $^5J(^{31}P-^1H)$ = 7.41 Hz, *m*-*CH*). $^{13}C\{^1H\}$ NMR (25 °C, CD_2Cl_2, 75.48 MHz): δ = 32.53 (d, $^5J(^{31}P-^{13}C)$ = 2.8 Hz, *o*-C(CH_3)$_3$), 33.63 (d, $^7J(^{31}P-^{13}C)$ = 4.7 Hz *p*-C(CH_3)$_3$), 35.21 (s, *p*-C(CH_3)$_3$), 36.60 (s, *o*-C(CH_3)$_3$), 122.52 (s, *m*-*CH*), 133.83 (aryl-*C*), 138.2 (dm, $^1J(^{13}C-^{19}F)$ = 257 Hz, aryl-*C*F), 144.6 (dm, $^1J(^{13}C-^{19}F)$ = 260 Hz, aryl-*C*F), 145.65 (aryl-*C*), 147.4 (dm, $^1J(^{13}C-^{19}F)$ = 250 Hz, aryl-*C*F), 149.16 (aryl-*C*). $^{31}P\{^1H\}$ NMR (25 °C, CD_2Cl_2, 121.51 MHz): δ = 361.6. $^{19}F\{^1H\}$ NMR (25 °C, CD_2Cl_2, 282.38 MHz): δ = −160.4 (m, *m*-*CF*), −147.3 (m, *p*-*CF*), −136.5 (m, *o*-*CF*). MS (EI, *m*/*z*, (>10%)): 41 (11), 57 (33), 69 (18), 77 (10), 110 (12), 198 (27) $[(C_6F_5)P]^+$, 246 (80) $[Mes^*H]^+$, 261 (36) $[Mes^*NH]^+$, 290 (100) $[Mes^*NP]^+$, 366 (18) $[(C_6F_5)_2PH]^+$, 493 (14), 550 (10). MS (ESI-TOF/MS): 262 $[Mes^*NH_2]^+$, 457 $[Mes^*NP(C_6F_5)]^+$. UV−vis: 592 nm.

Synthesis of 1,1-Bis(pentafluorophenyl)-2,4-bis(2,4,6-tri-*tert*-butylphenyl)-1,3-diphospha-2,4-diazene $(C_6F_5)_2PN(Mes^*)PNMes^*$ (2). To a stirred solution of C_6F_5Br (0.247 g, 1.0 mmol) in Et_2O (10 mL) *n*-BuLi (2.5 M, 0.4 mL, 1.0 mmol) is added dropwise at −80 °C over a period of 15 min. The solution of LiC_6F_5 is added quickly to a solution of Mes*NPCl (0.326 g, 1.0 mmol) in Et_2O (5 mL) at −80 °C by means of a PTFE tubing, resulting in a yellow suspension. After warming to ambient temperatures, the solvent is removed in vacuo and the residue is extracted with *n*-hexane (10 mL). Removal of solvent and drying in vacuo yields 0.427 g (0.467 mmol, 93.4%) of 1,1-bis(pentafluorophenyl)-2,4-bis(2,4,6-tri-*tert*-butylphenyl)-1,3-diphospha-2,4-diazene $(C_6F_5)_2PN(Mes^*)PNMes^*$ (**2**) as an orange solid.

Mp 123 °C. Anal. Calcd (found) for $C_{48}H_{58}F_{10}N_2P_2$ (914.92): C, 63.01 (62.99); H, 6.39 (6.81); N, 3.06 (2.82). ^{1}H NMR (25 °C, CD_2Cl_2, 300.13 MHz): δ = 1.25 (s, 18 H, C(CH_3)$_3$), 1.33 (s, 18 H, C(CH_3)$_3$), 1.37 (s, 18 H, C(CH_3)$_3$), 7.33 (s, 2 H, *m*-*CH*), 7.42 (s, 2 H, *m*-*CH*). $^{13}C\{^1H\}$ NMR (25 °C, CD_2Cl_2, 125.77 MHz): δ = 31.35 (s, *p*-C(CH_3)$_3$), 31.88 (s, *p*-C(CH_3)$_3$), 32.72 (s, *o*-C(CH_3)$_3$), 35.03 (s, *p*-C(CH_3)$_3$), 35.21 (s, *p*-C(CH_3)$_3$), 36.14 (s, *o*-C(CH_3)$_3$), 36.99 (s, *o*-C(CH_3)$_3$), 39.30 (s, *o*-C(CH_3)$_3$), 111.3 (dm, $^1J(^{31}P-^{13}C)$ = 71 Hz, *C*P), 123.05 (s, *m*-*CH*), 127.27 (s, *m*-*CH*), 136.86 (aryl-*C*), 138.2 (dm, $^1J(^{13}C-^{19}F)$ = 255 Hz, aryl-*C*F), 141.90 (m, $^2J(^{31}P-^{13}C)$ = 12 Hz, aryl-*C*N(P)P), 143.58 (aryl-*C*), 143.9 (dm, $^1J(^{13}C-^{19}F)$ = 257 Hz, aryl-*C*F), 149.0 (dm, $^1J(^{13}C-^{19}F)$ = 249 Hz, aryl-*C*F), 150.05 (aryl-*C*), 150.48 (aryl-*C*). $^{31}P\{^1H\}$ NMR (25 °C, CD_2Cl_2, 121.51 MHz): δ = 11.5 (m, *P*NPN), 290.2 (d, $^2J(^{31}P-^{31}P)$ = 6.7 Hz, PN*P*N). $^{19}F\{^1H\}$ NMR (25 °C, CD_2Cl_2, 282.38 MHz): δ = −161.4 (m, *m*-*CF*), −148.6 (m, *p*-*CF*), −120.8 (m, *o*-*CF*). MS (EI, *m*/*z*, (>10%)): 57 (69), 246 (60), 247 (11), 259 (12), 261 (18), 290 (31) $[Mes^*NP]^+$, 402 (97), 403 (30), 418 (100), 442 (17), 457 (56) $[Mes^*NP(C_6F_5)]^+$, 475 (12), 652 (14), 912 (10) $[M - 2H]^+$. UV−vis: 432.02 nm.

Crystals suitable for X-ray crystallographic analysis were obtained by cooling a saturated dichloromethane solution of **2** to −25 °C over a period of 10 h.

Synthesis of 1,3-Diiodo-2,4-bis(2,6-di-isopropylphenyl)-cyclo-1,3-diphospha-2,4-diazane (3I). To a stirred solution of 1,3-dichloro-2,4-bis(2,6-di-isopropylphenyl)-cyclo-1,3-diphospha-2,4-diazane (1.45 g, 3.0 mmol) in CH_2Cl_2 (15 mL) a solution of trimethylsilyl iodide (1.20 g, 6.0 mmol) in CH_2Cl_2 (10 mL) is added dropwise at ambient temperatures over a period of 30 min and stirred for 3 days. NMR studies show that just two-thirds of the dichloro-cyclo-diphospha-diazane is converted to the corresponding cyclo-diiodo compound. For

dx.doi.org/10.1021/ic200623x |*Inorg. Chem.* 2011, 50, 5784–5792

quick further conversion sodium iodide (0.45 g, 3.0 mmol) is added. Extraction with *n*-hexane and separation of P_2I_4 by fractional crystallization yields 1.74 g (2.61 mmol, 87%) of 1,3-diiodo-2,4-bis(2,6-diisopropylphenyl)-1,3-diphospha-2,4-diazane as a yellowish crystalline solid.

Mp 186 °C (dec.). Anal. Calcd (found) for $C_{24}H_{34}I_2N_2P_2$ (666.30): C, 43.26 (44.12); H, 5.14 (5.21); N, 4.20 (4.21). ^{1}H NMR (25 °C, $CDCl_3$, 300.13 MHz): δ = 1.34 (d, 24 H, $^3J(^1H-^1H)$ = 6.75 Hz, $CH(CH_3)_2$), 3.83 (sept, 4 H, $^5J(^1H-^{31}P)$ = 2.27 Hz, $CH(CH_3)_2$), $^3J(^1H-^1H)$ = 6.80 Hz, $CH(CH_3)_2$), 7.19 (d, 4 H, $^3J(^1H-^1H)$ = 7.50 Hz, (*m*-*CH*)), 7.30 (t, 2H, $^3J(^1H-^1H)$ = 7.61 Hz, (*p*-*CH*)). $^{13}C\{^1H\}$ NMR (25 °C, $CDCl_3$, 75.47 MHz): δ = 26.54 (s, $CH(CH_3)_2$), 29.27 (s, $CH(CH_3)_2$), 124.92 (*m*-CH), 129.05 (s, *p*-CH), 130.33 (t, $^3J(^{13}C-^{31}P)$ = 6.57 Hz, *o*-*C*), 149.5 (m, broad, *ipso*-*C*). $^{31}P\{^1H\}$ NMR (25 °C, $CDCl_3$, 121.49 MHz): δ = 265.0 (s). MS (CI^+, isobutane): 667 $[M + H]^+$, 539 $[M - I]^+$, 206 $[DippNP]^+$.

Crystals suitable for X-ray crystallographic analysis were obtained by storage of a saturated *n*-hexane solution of **3I** at ambient temperatures for 10 h.

Synthesis of 1,3-Bis(pentafluorophenyl)-2,4-bis(2,6-diisopropylphenyl)-cyclo-1,3-diphospha-2,4-diazane [DippNP-(C_6F_5)]$_2$ (3). To a stirred solution of $[DippNPX]_2$ (X = Cl 0.242 g, 0.5 mmol; X = I 0.333 g, 0.5 mmol) in CH_2Cl_2 (5 mL) a suspension of AgC_6F_5 (0.275 g, 1.0 mmol) in CH_2Cl_2 (15 mL) is added dropwise at −80 °C over a period of 20 min. The resulting brownish solution is slowly warmed to ambient temperatures and stirred for three hours resulting in a yellow suspension. The solvent is removed in vacuo and the residue is extracted with *n*-hexane (10 mL) and filtered. Removal of solvent and drying in vacuo yields for X = Cl 0.244 g (0.327 mmol, 65%) and for X = I 0.284 g (0.381 mmol, 76%) of 1,3-bis(pentafluorophenyl)-2,4-bis(2,6-di-isopropylphenyl)-cyclo-1,3-diphospha-2,4-diazane [DippNP-(C_6F_5)]$_2$ (**3**) as yellow crystals.

Mp 133 °C. Anal. Calcd (found) for $C_{36}H_{34}F_{10}N_2P_2$ (746.60): C, 57.91 (57.81); H, 4.59 (4.72); N, 3.75 (3.50).^{1}H NMR (25 °C, CD_2Cl_2, 300.13 MHz): δ = 1.08 (d, 12 H, $^3J(^1H-^1H)$ = 6.66 Hz, $CH(CH_3)_2$), 1.18 (d, 12 H, $^3J(^1H-^1H)$ = 6.80 Hz, $CH(CH_3)_2$), 3.91 (septm, 4 H, $^5J(^{31}P-^1H)$ = 2.27 Hz, $CH(CH_3)_2$), $^3J(^1H-^1H)$ = 6.80 Hz, $CH(CH_3)_2$), 7.10 (m, 6 H, (aryl-*CH*)). $^{13}C\{^1H\}$ NMR (25 °C, CD_2Cl_2, 75.47 MHz): δ = 25.59 (t, $^5J(^{13}C-^{31}P)$ = 2.74 Hz, $CH(CH_3)_2$), 29.19 (t, $^4J(^{13}C-^{31}P)$ = 8.24 Hz, $CH(CH_3)_2$), 125.08 (s, *m*-*CH*), 126.82 (s, *p*-*CH*), 132.78 (aryl-*C*), 147.26 (aryl-*C*), 138 (dm, $^1J(^{13}C-^{19}F)$ = 257 Hz, aryl-CF), 143 (dm, $^1J(^{13}C-^{19}F)$ = 239 Hz, aryl-CF), 146 (dm, $^1J(^{13}C-^{19}F)$ = 242 Hz, aryl-CF). $^{31}P\{^1H\}$ NMR (25 °C, CD_2Cl_2, 121.49 MHz): δ = 264.2 (m). $^{19}F\{^1H\}$ NMR (25 °C, CD_2Cl_2, 282.40 MHz): δ = −160.9 (m, *m*-*CF*), −149.2 (m, *p*-*CF*), −134.1 (m, *o*-*CF*). MS (CI^+, isobutane): 747 $[[DippNP(C_6F_5)]_2 + H]^+$, 430 $[DippNP(C_6F_5) + i\text{-}Pr - H]^+$, 416 $[DippNP(C_6F_5) + i\text{-}Pr]^+$, 373 $[DippNP(C_6F_5)]^+$.

Crystals suitable for X-ray crystallographic analysis were obtained by storage of a saturated benzene solution of **3** at ambient temperatures for 10 h.

Synthesis of *N*-(2,4,6-Tri-*tert*-butylphenyl)imino(pentafluorophenyl)phosphane Iron Tetracarbonyl Adduct Mes*NP(C_6F_5)·Fe(CO)$_4$ (5). To a stirred suspension of $Fe_2(CO)_9$ (0.363 g, 1.0 mmol) in *n*-hexane (8 mL), a solution of Mes*NPC_6F_5 (0.457 g, 1.0 mmol) in *n*-hexane (10 mL) is added quickly at −50 °C without stirring. The resulting brown suspension is warmed to ambient temperatures, stirred for 5 h, and filtered (F4). The resulting red solution is concentrated to an approximate volume of 5 mL and cooled to 5 °C for 10 h, resulting in the deposition of dark red crystals which can be identified as $Fe_3(CO)_{12}$ by X-ray-crystallographic analysis. The supernatant is separated and further concentrated to give *N*-(2,4,6-tri-*tert*-butylphenyl)imino(pentafluorophenyl)phosphane iron tetracarbonyl adduct Mes*NP(C_6F_5)·Fe(CO)$_4$ (**5**) as red crystals. Yield: 0.52 g (0.82 mmol, 82%).

Mp 103 °C (dec.). Anal. Calcd (found) for $C_{28}H_{29}F_5FeNO_4P$ (625.34): C, 53.78 (53.74); H, 4.67 (4.55); N, 2.24 (2.14). ^{1}H NMR (25 °C, CD_2Cl_2, 300.13 MHz): δ = 1.28 (s, 9 H, *p*-$C(CH_3)_3$), 1.43 (s, 18 H, *o*-$C(CH_3)_3$), 7.32 (d, 2 H, $^5J(^{31}P-^1H)$ = 2.5 Hz, *m*-*CH*). $^{13}C\{^1H\}$ NMR (25 °C, CD_2Cl_2, 75.48 MHz): δ = 31.74 (s, *p*-$C(CH_3)_3$), 32.05 (s, *o*-$C(CH_3)_3$), 35.12 (d, $^6J(^{31}P-^{13}C)$ = 1.1 Hz, *p*-$C(CH_3)_3$), 36.64 (d, $^4J(^{31}P-^{13}C)$ = 1.9 Hz, *o*-$C(CH_3)_3$), 122.99 (d, $^4J(^{31}P-^{13}C)$ = 4.7 Hz, *m*-*CH*), 138.00 (aryl-*C*), 146.23 (aryl-*C*), 208.93 (d, $^2J(^{31}P-^{13}C)$ = 9.9 Hz, *CO*). $^{31}P\{^1H\}$ NMR (25 °C, CD_2Cl_2, 121.51 MHz): δ = 300.6. $^{19}F\{^1H\}$ NMR (25 °C, CD_2Cl_2, 282.38 MHz): δ = −159.1 (m, *m*-*CF*), −148.6 (m, *p*-*CF*), −132.8 (m, *o*-*CF*). MS (EI, *m*/*z*, (>10%)): 41 (13), 57 (37), 246 (18) [Mes*]$^+$, 260 (11), 290 (25) [Mes*NP]$^+$, 297 (11), 313 (18), 315 (43), 440 (13), 513 (100) [Mes*NP(Fe)C_6F_5]$^+$, 541 (17) [Mes*NP(FeCO)C_6F_5]$^+$, 625 (10) $[M]^+$.

Crystals suitable for X-ray crystallographic analysis were obtained by storage of a saturated *n*-hexane solution of **5** at ambient temperature for 10 h.

■ ASSOCIATED CONTENT

Supporting Information. This material is available free of charge via the Internet at http://pubs.acs.org.

■ AUTHOR INFORMATION

Corresponding Author
*E-mail: axel.schulz@uni-rostock.de.

■ ACKNOWLEDGMENT

We are indepted to Dr. D. Michalik and J. Thomas (University of Rostock). Generous support by the University of Rostock is gratefully acknowledged. We would like to thank the Deutsche Forschungsgemeinschaft (SCHU 1170/4-1) for financial support.

■ REFERENCES

(1) (a) *Multiple Bonds and Low Coordination in Phosphorus Chemistry*; Regitz, M., Scherer, O. J., Eds.; Weinheim, 1990. (b) Weber, L. *Chem. Rev.* **1992**, *92*, 1839. (c) Weber, L. *Chem. Ber.* **1996**, *129*, 367.

(2) Niecke, E.; Gudat, D. *Angew. Chem.* **1991**, *103*, 251–270. *Angew. Chem., Int. Ed. Engl.* **1991**, *30* (3), 217–37 and references therein.

(3) Niecke, E.; Flick, W. *Angew. Chem.* **1973**, *85* (13), 586–587. *Angew. Chem., Int. Ed. Engl.* **1973**, *12*, 585–586.

(4) Niecke, E.; Nieger, M.; Reichert, F. *Angew. Chem.* **1988**, *12*, 1781–1782. *Angew. Chem., Int. Ed.* **1988**, *27*, 1715–1716.

(5) (a) Burford, N.; Clyburne, J. A. C.; Chan, M. S. W. *Inorg. Chem.* **1997**, *36*, 3204–3206. (B) Burford, N.; Cameron, T. S.; Conroy, K. D.; Ellis, B.; Lumsden, M. D.; Macdonald, C. L. B.; McDonald, R.; Phillips, A. D.; Ragogna, P. J.; Schurko, R. W.; Walsh, D.; Wasylishen, R. E. *J. Am. Chem. Soc.* **2002**, *124*, 14012–14013.

(6) Balakrishna, M. S.; Eisler, D. J.; Chivers, T. *Chem. Soc. Rev.* **2007**, *36*, 650–664and references therein.

(7) Lehmann, M.; Schulz, A.; Villinger, A. *Struc. Chem.* **2011**, *22* (1), 35–43.

(8) (a) Villinger, A.; Westenkirchner, A.; Wustrack, R.; Schulz, A. *Inorg. Chem.* **2008**, *47*, 9140–9142. (b) Schulz, A.; Villinger, A. *Eur. J. Inorg. Chem.* **2008**, 4199–4203. (c) Hubrich, Ch.; Michalik, D.; Schulz, A.; Villinger, A. *Z. Anorg. Allg. Chem.* **2008**, 1403–1408. (d) Schaffrath, M.; Villinger, A.; Michalik, D.; Rosenthal, U.; Schulz, A. *Organometallics* **2008**, *27*, 1393–1398. (e) Kowalewski, M.; Krumm, B.; Mayer, P.; Schulz, A.; Villinger, A. *Eur. J. Inorg. Chem.* **2007**, 5319–5322. (f) Fischer, G.; Herler, S.; Mayer, P.; Schulz, A.; Villinger, A.; Weigand, J. J. *Inorg. Chem.* **2005**, *44*, 1740–1751. (g) Götz, N.; Herler, S.; Mayer, P.; Schulz, A.; Villinger, A. *Eur. J. Inorg. Chem.* **2006**, 2051–2057.

(9) Burford, N.; Clyburne, J. A. C.; Bakshi, P. K.; Cameron, T. S. *Organometallics* **1995**, *14*, 1578–1585.
(10) (a) Fild, M.; Hollenberg, I.; Glemser, O. *Naturwissenschaften* **1967**, *54* (4), 89–99. (b) Ang, H. G.; Miller, J. M. *Chem. Ind. (London)* **1966**, 945.
(11) Detsch, R.; Niecke, E.; Nieger, M.; Reichert, F. *Chem. Ber.* **1992**, *125*, 321–330.
(12) Kuprat, M.; Kuzora, R.; Lehmann, M.; Schulz, A.; Villinger, A.; Wustrack, R. *J. Organomet. Chem.* **2010**, *695*, 1006–1011.
(13) (a) Bartlett, R. A.; Rasika Dias, H. V.; Flynn, K. M.; Olmstead, M. M.; Power, P P. *J. Am. Chem. Soc.* **1987**, *109*, 5699–5703. (b) Flynn, K. M.; Olmstead, M. M.; Power, P. P. *J. Am. Chem. Soc.* **1983**, *105*, 2085–2086. (c) Flynn, K. M .; Murray, B. D.; Olmstead, M. M.; Power, P. P. *J. Am. Chem. Soc.* **1983**, *105*, 7460–7461. (d) Flynn, K. M.; Hope, H.; Murray, B. D.; Olmstead, M M.; Power, P. P. *J. Am. Chem. Soc.* **1983**, *105*, 7750–7751. (e) Flynn, K. M.; Bartlett, R. A; Olmstead, M. M.; Power, P. P. *Organometallics* **1986**, *5*, 813–815.
(14) References for RP═PR species: (a) Yoshifuji, M.; Shima, I.; Inamoto, N.; Hirotsu, K.; Higuchi, T. *J. Am. Chem. Soc.* **1981**, *103*, 4587–4589. (b) Mathey, F. In *Multiple Bonds and Low Coordination in Phosphorus Chemistry*; Regitz, M.; Scherer, O. J., Eds.; Thieme Verlag: Stuttgart, 1990; pp 33− 47. (c) Power, P. P. *J. Chem. Soc., Dalton. Trans.* **1998**, 2939–2951. (d) Twamley, B.; Haubrich, S. T.; Power, P. *Adv. Organomet. Chem.* **1999**, 1. (e) Clyburne, J. A. C.; McMullen, N. *Coord. Chem. Rev.* **2000**, *210*, 73–99.
(15) Values have been corrected according to the Schomaker−Steveson equation for highly polar bonds: $d_{AB} = r_A + r_B - c|\chi_A - \chi_B|$, Holleman Wiberg, *Lehrbuch der Anorganischen Chemie*, 101. Aufl., Walter de Gruyter, 1995, Anhang V.Holleman Wiberg, Lehrbuch der Anorganischen Chemie, 102. Aufl., Walter de Gruyter, Berlin, 2007, Anhang IV
(16) (a) Glendening, E. D.; Reed, A. E.; Carpenter, J. E.; Weinhold, F. NBO Version 3.1; (b) Reed, A. E.; Curtiss, L. A.; Weinhold, F. *Chem. Rev.* **1988**, *88*, 899–926.
(17) Flynn, K. M.; Murray, B. D.; Olmstead, M. M.; Power, P. P. *J. Am. Chem. Soc.* **1983**, *105*, 7460–7461.
(18) Stahl, L. *Coord. Chem. Rev.* **2000**, *210*, 203–250 and references therein.
(19) (a) Doyle, E. L.; Riera, L.; Wright, D. S. *Eur. J. Inorg. Chem.* **2003**, 3279–3289. (b) Beswick, M. A.; Wright, D. S. *Coord. Chem. Rev.* **1998**, *176*, 373–406.
(20) (a) Burford, N.; Cameron, T. S.; Conroy, K. D.; Ellis, B.; Macdonald, C. L. B.; Ovans, R.; Phillips, A. D.; Ragogna, P. J.; Walsh, D. *Can. J. Chem.* **2002**, *80*, 1404–1409. (b) Burford, N.; Cameron, T. S.; Macdonald, C. L. B.; Robertson, K. N.; Schurko, R.; Walsh, D. *Inorg. Chem.* **2005**, *44*, 8058–8064.